

Seismic anisotropy and salt detection: A physical modelling study

Zandong Sun, R. James Brown, and Don C. Lawton

ABSTRACT

Salt has been of considerable interest in petroleum exploration in western Canada. Identifying and separating salt remnants from reefs on seismic sections is of great concern for petroleum explorationists. In this physical modelling study, zero-offset transmission experiments have been undertaken on three different types of salt and salt-correlated anhydrite. Velocity of a salt sample under different pressure and temperature also has been tested. Pure salt and recrystallized salt have been found to exhibit shear-wave splitting. However, impure salts (salt mixed with clay, sands, etc.) show no shear-wave splitting. Theoretically, the wave (group-velocity) surfaces indicate that there should be only a single shear-wave velocity along principal (symmetry) axes. The minimum value of P -wave velocity and the maximum difference between qSV and qSH velocities are in the (1,1,0) direction in the first quadrant. Seismic anisotropy should be able to help us to identify pure salt and recrystallized salt, and anisotropy in anhydrite may provide indirect information about the evaporite sequence. There is little velocity change in salt with changes in pressure and temperature.

INTRODUCTION

Devonian salts play a very important role in oil accumulation and distribution in western Canada (Edmunds, 1980; Anderson and Brown, 1991). The Athabasca anticline, the largest single liquid oil accumulation in the world indicated by new data, is a trap structure caused by Devonian salt removal (Masters, 1984).

Geologically, as seawater evaporates, the concentration of the carbonates, sulphates and chlorides increases to the point where one or more salts will precipitate. In the depositional sequence of evaporites, calcite and gypsum are the first salts to precipitate, followed by halite. Under subsurface conditions, gypsum is replaced by anhydrite due to increased pressure and temperature. This sequence is very common in the Devonian of western Canada where salt is usually correlated with anhydrite (Figure 1). Salt crystals grow in certain trends where salt was originally deposited in a stable environment. The thicker and purer the salt unit stratigraphically, the stabler was the environment of deposition. It is quite common in western Canadian Devonian units for salt to have been deposited over 100 m thick originally (Meijer Drees, 1986). Crystal lattices in recrystallized salt are rearranged in certain ways due to the paleogeothermal gradient and pressure in the region.

An experimental study has been done on 17 salt and anhydrite samples which were collected from six different areas in Alberta, Canada. This study concerns seismic anisotropy, resulting from stress-induced crystal alignment, of salt and salt-correlated anhydrite for purposes of identifying salt and, for example, separating remnants of it from reefs on seismic sections. Theoretical wave surfaces have also been computed.

ANISOTROPY THEORY AND WAVE SURFACES

The waves propagating in anisotropic elastic media can be described by the well known Kelvin-Christoffel equation:

$$(n_i n_j c_{ijkl} - \rho v^2 \delta_{jk}) P_k = 0 \quad (1)$$

where Einstein's summation convention is employed, n_i is the unit vector normal to the wavefront, c_{ijkl} is the tensor of elastic stiffnesses, ρ is the density (for salt $\rho = 2.165$ at 25°C), v is the phase velocity, δ_{jk} is the Kronecker delta, and P_k is the particle-motion or polarization vector. It is indicated by equation (1) that if the direction of propagation (n_i) and elastic stiffnesses are known, then the magnitude of phase velocity (v) and slowness can be calculated through computing the eigenvalues of (1).

The fourth-order tensor c_{ijkl} can be written as a second-order (6×6) symmetric matrix, due to symmetry (Musgrave, 1970; Crampin, 1981; Thomsen, 1986; Winterstein, 1990). In the case of cubic symmetry, only three independent stiffnesses have nonzero values (Musgrave, 1970; Miller and Musgrave, 1956):

$$c_{11} = c_{22} = c_{33}; \quad c_{12} = c_{13} = c_{23}; \quad c_{44} = c_{55} = c_{66}. \quad (2)$$

In the principal direction $n_i = (1,0,0)$, equation (1) gives solutions:

$$c_{11} = \rho v_{11}^2; \quad c_{44} = \rho v_{12}^2 = \rho v_{13}^2 \quad (3)$$

where v_{ij} is the phase velocity, also equal to the group velocity due to the symmetry. The wave propagation direction is denoted by i , while j refers to the particle motion direction. The relationship between phase velocity and group velocity has been discussed, for example, by Thomsen (1986) and Brown et al. (1991). In the direction $n_i = (1,1,0)$, equation (1) gives solution for P -wave velocity:

$$\rho v_{44} = \frac{1}{2}(c_{11} + c_{12} + 2c_{44}). \quad (4)$$

In order to deduce the stiffnesses, velocity measurements have been carried out in specific directions through a salt sample (measuring 115×115×100 mm). The parameters are listed in Table 1. The phase-velocity surfaces and slowness on section $\{0,0,1\}$ were computed by applying these parameters (Figures 2a and b). Components of the group velocity, V_i , were computed using:

$$V_i = \frac{c_{ijk} p_l D_{jk}}{\rho D_{qq}} \quad (5)$$

after Kendall and Thomson (1989), where D_{jk} is a cofactor of the matrix $c_{ijk} p_l D_{jk} / \rho - \delta_{jk}$, and p_l is slowness. The first quadrant of wave surfaces (or group-velocity surfaces) on the

section is illustrated in Figure 2c. These are generated from slowness surfaces and represent theoretical wavefronts at unit time. As indicated by Figure 2c, the qSH wavefront is nearly circular and the maximum shear-velocity difference is approximately 20% in the (1,1,0) direction; also, P -wave velocity in that direction approaches a minimum value. The points where two shear waves have same velocity are the principal or symmetry axes. This agrees with the experimentally observed results (Table 1).

Table 1. Salt Anisotropy Parameters

V_p (km/s)		V_s (km/s)		c_{11} *	c_{12} *	c_{44} *
(1,0,0)	(1,1,0)	(1,0,0)	(1,1,0)	46.992	14.025	12.269
4.6589	4.4451	2.3806	S1: 2.8327			
			S2: 2.3800			

* unit: 10^{11} dyne/cm²

EXPERIMENTS AND RESULTS

The experiments were set up with P -wave and S -wave transducers as both sources and receivers. Both types of transducers are flat-faced cylindrical contact transducers with an active element 12.6 mm in diameter. Amplified data were sampled every 50 ns using a Nicolet digital oscilloscope connected, through an IBM-XT, which controls the experiment, to a Perkin-Elmer 3240 seismic processing system for storage. The frequency scaling was 10,000:1; distance and time scaling were 1:10,000. Each trace contains 4000 samples and it was stored on disk in SEG-Y format. The record length was 2.0 s (scaled).




Shear-wave splitting experiment

In this experiment, the sample was placed between two fixed shear-wave transducers which were aligned with parallel polarizations. The sample was rotated between the transducers and a pointer on the sample was used to determine the azimuth of the sample with respect to a fixed circular protractor (Figure 3). Data were recorded every 11.25° per trace (from 0° to 360°) with 32 traces per record. Similar experiments were carried out by Tatham et al. (1987) for the study of fracture-induced shear-wave splitting and Cheadle et al. (1991) in an orthorhombic-anisotropy model study.

The transmission records for propagation through a pure salt crystal sample (where a principal axis is the same as rotation axis) is shown in Figure 4a. The plot shows that there is no time shift of shear-wave first arrivals in all the polarization directions. It indicates that the results from actual observations agree with the theoretical wave surfaces, i.e. there is only a single shear-wave velocity along the principal axis. The experimental result from a recrystallized salt core sample is shown in Figure 4b. It is shown in the plot that the shear-wave first arrival traveltimes change as the polarization changes. The change in shear-wave velocity is 4.8% (Table 2). The result for a pure salt core sample, for which crystal sizes range from 1 to 6 mm, is shown in Figure 4c. The shear-wave velocity change is 4.6% (Table 2). However, impure salt (mixed uniformly with clay), with crystal sizes from 1 to 10 mm, does not show shear-wave splitting (Figure 4d). The P , $S1$, $S2$

velocities measured from different samples are summarized in Table 2. These values are group velocities based on the transit time. The time picks used to calculate the velocities were made directly on the digital oscilloscope for maximum accuracy.

Table 2. Velocities on different salt samples

samples	wave propagation	length (mm)	<i>P</i> wave velocity (km/s)	<i>S</i> 1 velocity (km/s)	<i>S</i> 2 velocity (km/s)	<i>S</i> -waves change (%)
pure salt crystal	direction (1,1,0)	155.80	4.4451	2.8327	2.3800	20.1
pure salt		95.90	4.4195	2.6863	2.5677	4.6
recrystallized pure salt		279.93	4.5076	2.6112	2.4927	4.8
salt mixed with clay		145.43	4.3803	2.5807		0

Anhydrite core samples were also tested. The results from a pure finely crystallized anhydrite sample (88 mm in length) are shown in Figure 5a; those from dolomitic anhydrite (397 mm in core length) are shown in Figure 5b. Both show shear-wave splitting and are regarded to be anisotropic.

Velocity variation with pressure and temperature

The variation of velocity under pressure and temperature changes was also studied. Plots of *P*-wave and faster-shear-wave velocity versus increasing pressure and temperature from a salt sample are shown in Figure 6. The velocity of the *P*-wave and shear-wave exhibits a slight increase with increasing pressure and temperature. It indicates that velocities measured in the laboratory are probably close to those in the subsurface.

CONCLUSION

This study has shown that recrystallized salt and pure salt are anisotropic. The maximum velocity difference between fast-shear- and slow-shear-wave velocities, observed from cores in the laboratory, is around 5%. Except on principal symmetry axes shear-wave splitting can be observed. The maximum shear-velocity difference is in the (1,1,0) direction. The *P*-wave velocity is also slowest in this direction. Impure salt shows isotropic behaviour. Anisotropy in anhydrite can provide information to aid in the identification of evaporite sequences. The salt velocities observed in the laboratory are believed to be very close to the actual velocities in the subsurface.

ACKNOWLEDGEMENTS

This research was supported by the CREWES project at The University of Calgary. The cooperation of the Energy Resources Conservation Board (ERCB) Core Research Centre, in particular, permission to loan and in some cases to cut drill core, is gratefully acknowledged. Dr N.C. Meijer Drees is thanked for his assistance in the salt subdivision

and classification. Group velocities were calculated using a program provided by Dr. D.W.S. Eaton (CREWES). Finally, we thank Mr. D.T. Easley for many helpful suggestions and Messrs. M.B. Bertram and E.V. Gallant for their expert help in the laboratory.

REFERENCES

- Anderson, N.L., and Brown, R.J., 1991, A seismic analysis of Black Creek and Wabamun salt collapse features, western Canadian sedimentary basin: *Geophysics*, **56**, 6 18–627.
- Brown, R.J., Lawton, D.C., and Cheadle, S.P., 1991, Scaled physical modelling of anisotropic wave propagation: multioffset profiles over an orthorhombic medium: *Geophys. J. Internat.*, **107**, 693–702.
- Cheadle, S. P., Brown, R.J., and Lawton, D.C., 1991, Orthorhombic anisotropy: A physical seismic modeling study: *Geophysics*, **56**, 1603–1613.
- Crampin, S., 1981, A review of wave motion in anisotropic and cracked elastic-media: *Wave Motion*, **3**, 343–391.
- Edmunds, R.H., 1980, Salt removal and oil entrapment: *Can. Soc. Petr. Geol., Mem.* **6**, 988 (abstract).
- Kendall, J-M., and Thomson, C.J., 1989, A comment on the form of the geometrical spreading equations, with some numerical examples of seismic ray tracing in inhomogeneous, anisotropic media: *Geophys. J. Int.*, **99**, 401–413.
- Masters, J.A. et al., 1984, Elmworth – Case Study of a Deep Basin Gas Field: *Amer. Assoc. Petr. Geol., Mem.* **38**.
- Meijer Drees, N.C., 1986, Evaporitic Deposits of Western Canada: *Geol. Surv. Can., Paper* 85–20.
- Miller, G.F., and Musgrave, M.J.P., 1956, On the propagation of elastic waves in aeolotropic media. III. Media of cubic symmetry: *Proc. Roy. Soc., A*, **236**, 352–383.
- Musgrave, M.J.P., 1970, *Crystal Acoustics*: Holden-Day, San Francisco.
- Tatham, R.H., Mathews, M.D., Sekharan, K.K., Wade, C., and Liro, L.M., 1987, A physical model study of shear-wave splitting and fracture intensity: *57th Ann. Internat. Mtg. Soc. Expl. Geophys., Expanded Abstracts*, 642–645.
- Thomsen, L., 1986, Weak elastic anisotropy: *Geophysics*, **51**, 1954–1966.
- Winterstein, D.F., 1990, Velocity anisotropy terminology for geophysicists: *Geophysics*, **55**, 1070–1088.

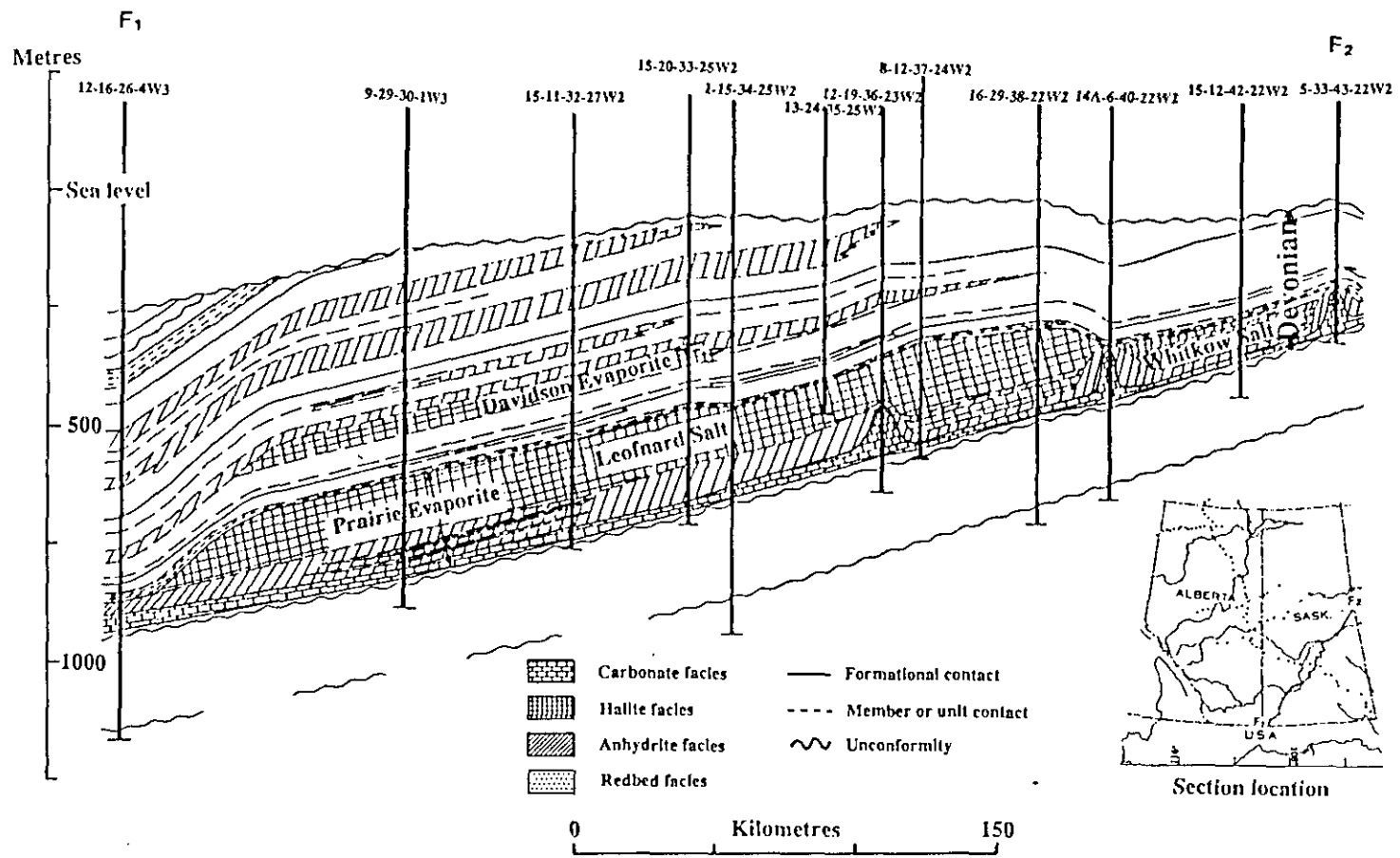
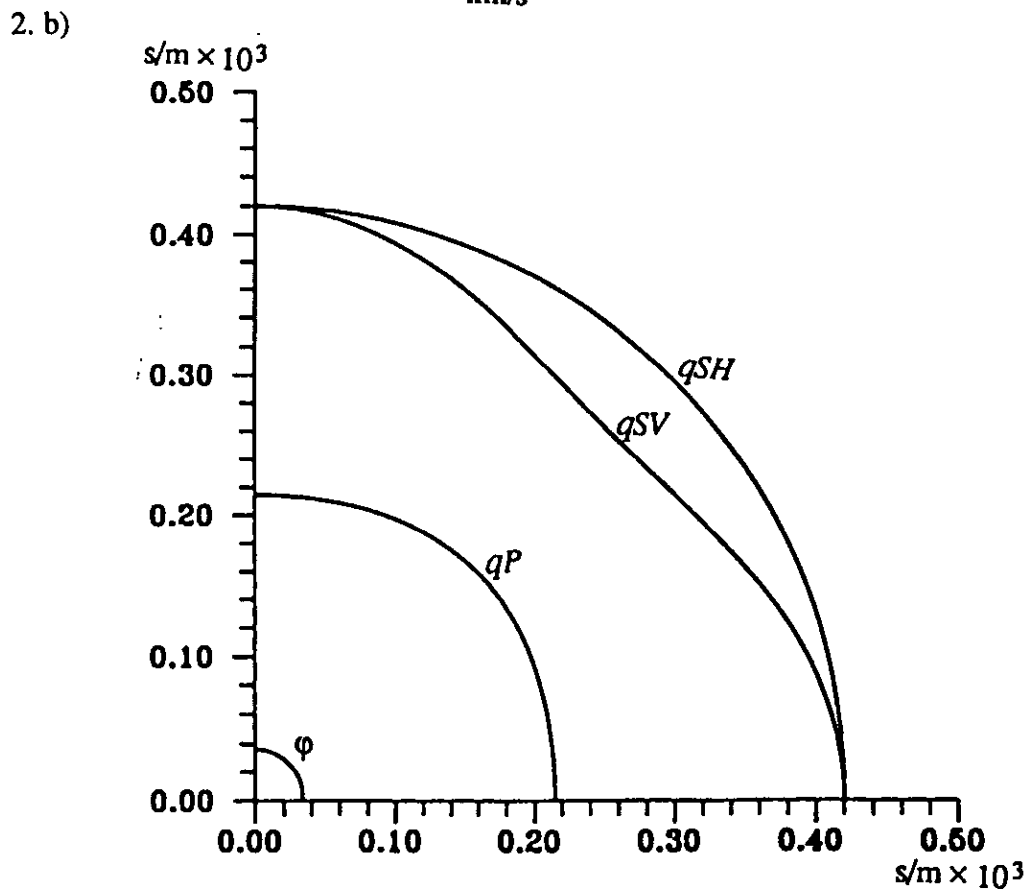
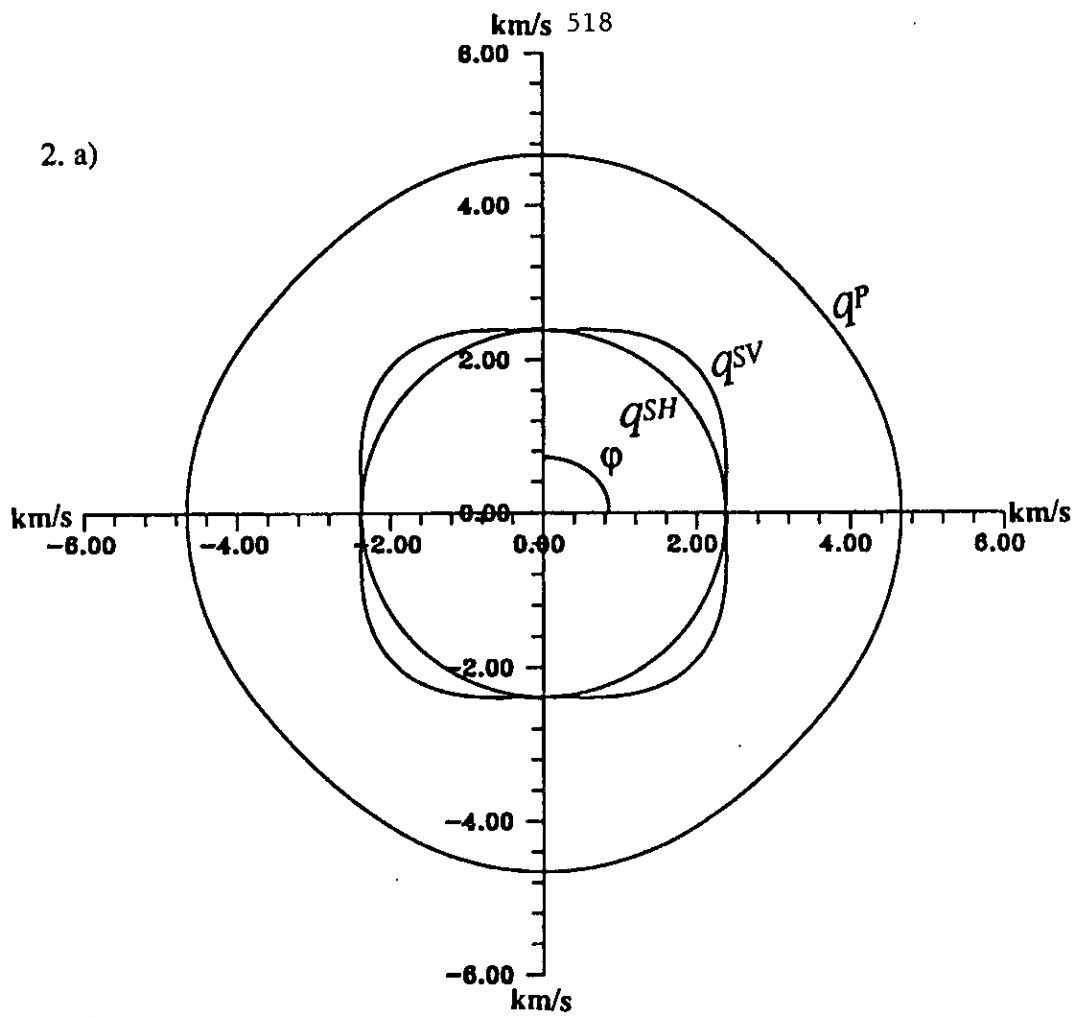


FIG. 1 Typical Devonian evaporite section in western Canada (modified after Meijer Drees, 1986).



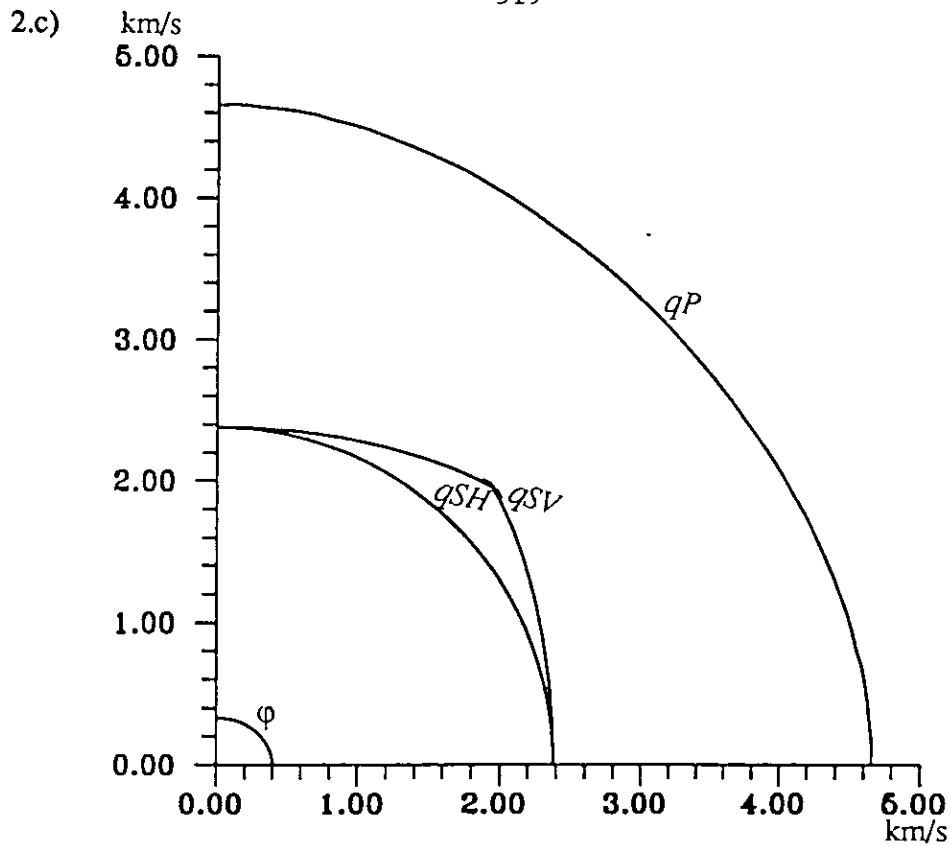


FIG. 2 Phase-velocity surfaces (a), phase-slowness (b), and group velocity (wave) surfaces (c) on section $\{0,0,1\}$ for salt.

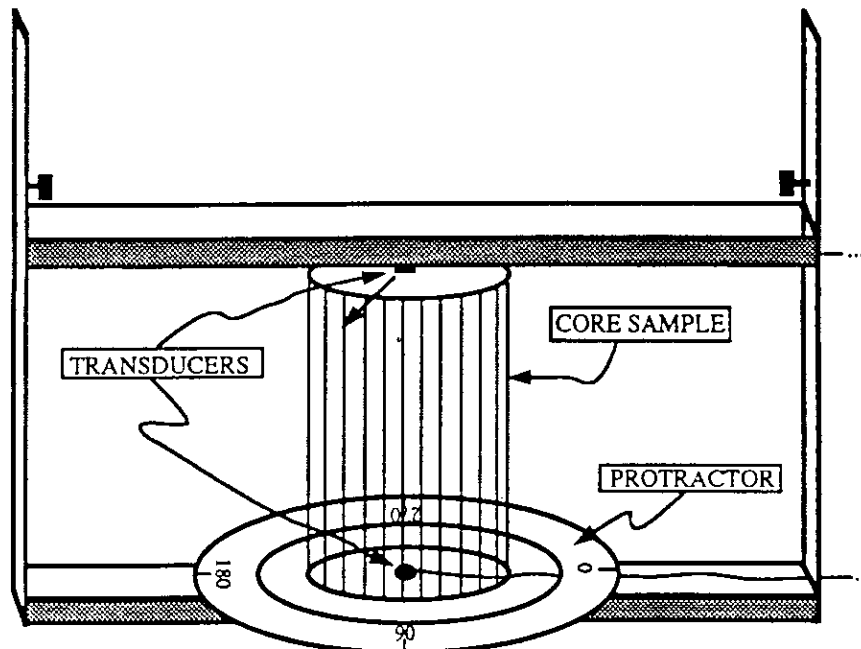
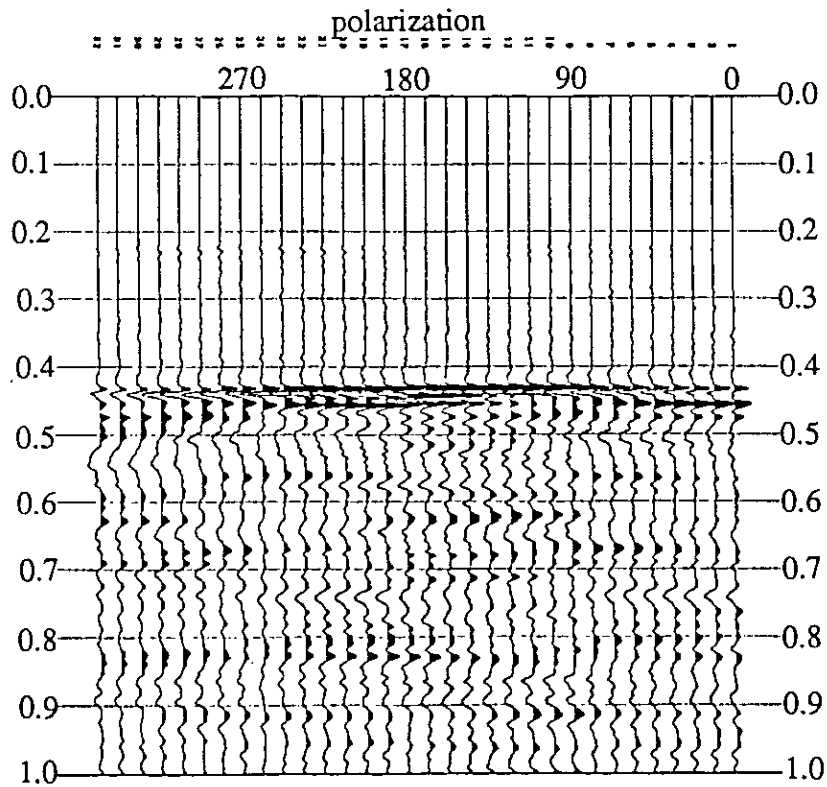
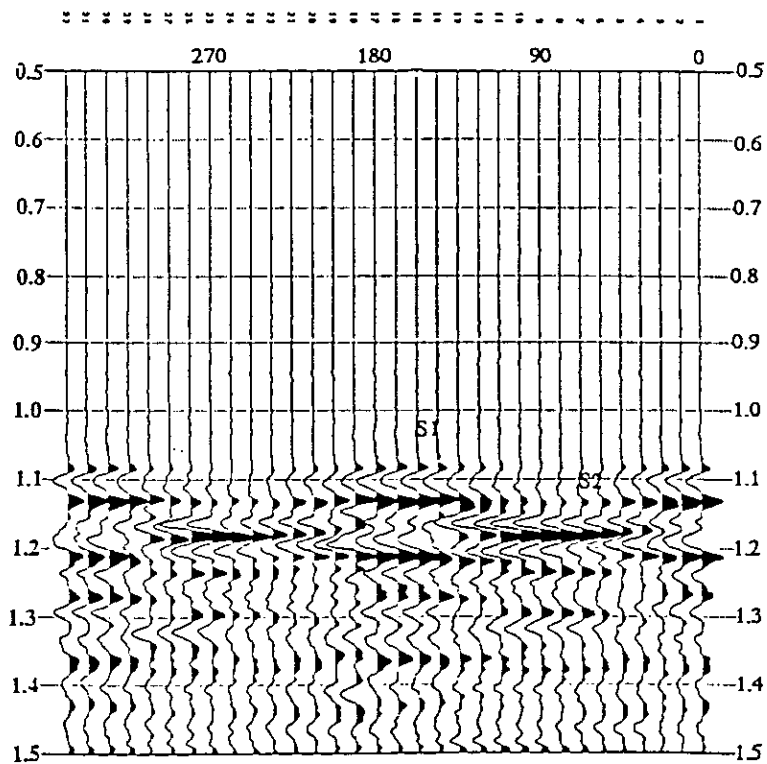


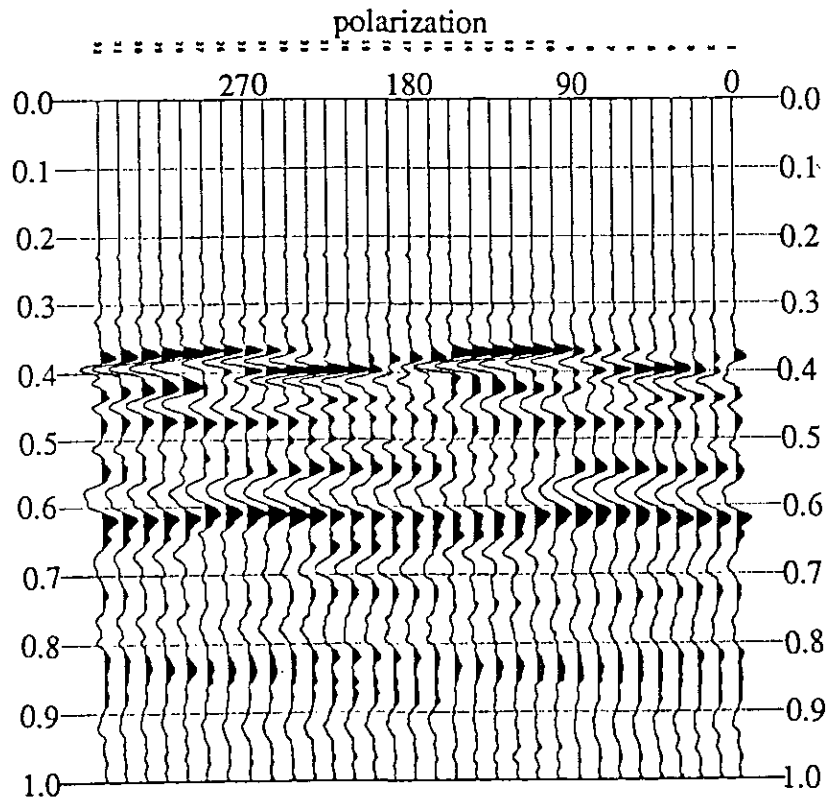
FIG. 3 Schematic diagram showing shear-wave splitting zero-offset transmission experiment apparatus. Sample is located between two shear-wave transducers with mutually parallel polarization. The sample is rotated while the transducers remain fixed. A circular protractor scale is used to determine the azimuth of rotation.



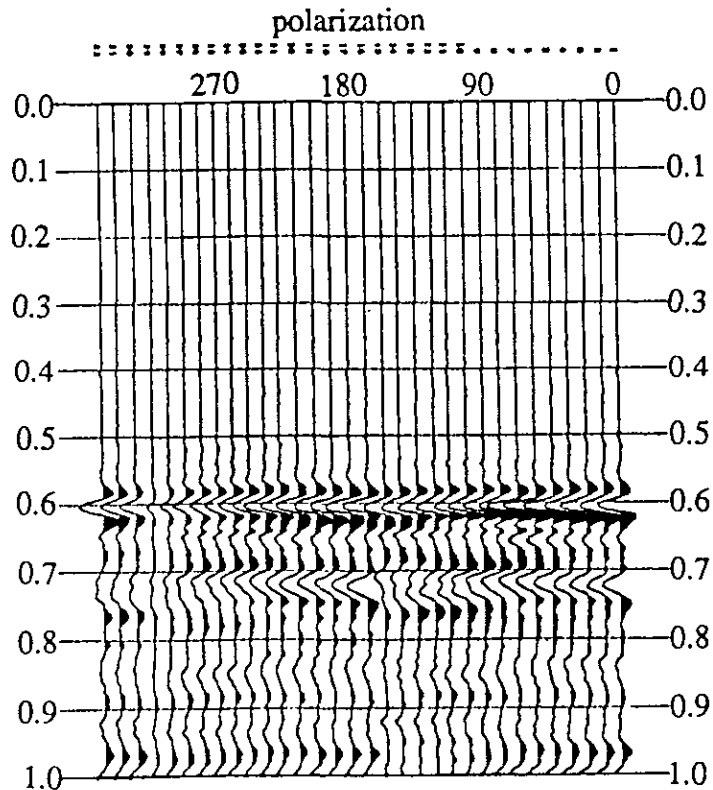
a) experiment on salt crystal, rotation axis is a principle axis of symmetry (approx.)
on salt crystal; sample length: 100.4 mm.



b) experiment on recrystallized salt sample; sample length: 279.9 mm.



c) experiment on a pure salt sample (crystal size: 1-6 mm); sample length: 95.9 mm.



d) experiment on impure salt sample mixed uniformly with clay; sample length: 145.4 mm.

FIG. 4 Plots of zero-offset transmission experiments with different polarization on different salt samples. Both shear-wave transducers were rotated from at increments of 11.25° .

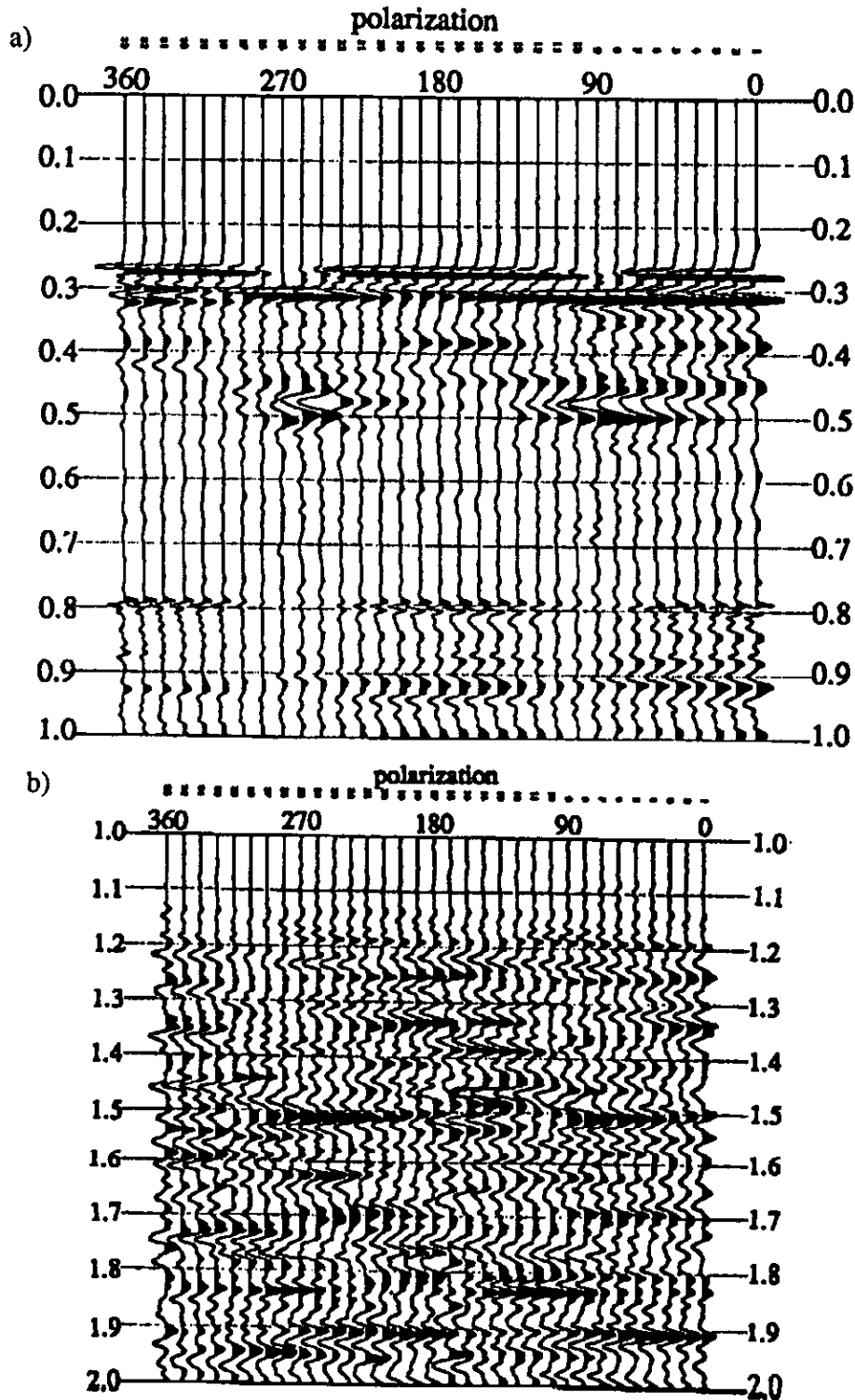


FIG. 5 Plots of zero-offset transmission experiment with different polarization on different anhydrite samples. Both shear-wave transducers were rotated from 0° to 360° at increments of 11.25° .

a) experiment on a pure anhydrite sample (fine crystal size); sample length: 88.0 mm.

b) experiment on dolomitic anhydrite sample (fine crystal size) mixed with clay; sample length: 396.4 mm.

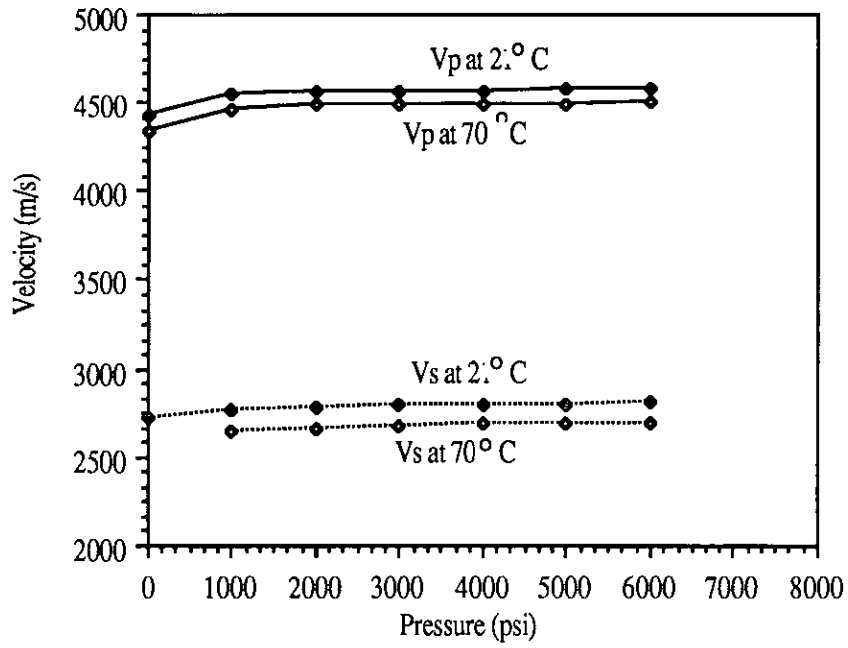


FIG. 6 Velocity versus pressure and temperature in salt F